Published in final edited form as:

Fertil Steril. 2020 November ; 114(5): 1085–1096. doi:10.1016/j.fertnstert.2020.05.036.

HMGA2-mediated tumorigenesis through angiogenesis in leiomyoma

Yinuo Li, M.D.[a], **Wenan Qiang, Mb., Ph.D.**[b], **Brannan Brooks Griffin, M.D.**[a], **Tingting Gao, M.D.**[a], **Debabrata Chakravarti, Ph.D.**[b], **Serdar Bulun, M.D.**[b], **J. Julie Kim, Ph.D.**[b], **Jian-Jun Wei, M.D.**[a,b]

[a]Department of Pathology and Feinberg School of Medicine, Northwestern University, Chicago, Illinois

[b]Department of Obstetrics and Gynecology, Feinberg School of Medicine, Northwestern University, Chicago, Illinois

Abstract

Objective: To study the role of HMGA2 in promoting angiogenesis in uterine leiomyoma (LM).

Design: This study involved evaluation of vessel density and angiogenic factors in leiomyomas with *HMGA2* overexpression; examining angiogenic factor expression and AKT signaling in myometrial and leiomyoma cells by introducing *HMGA2* overexpression in vitro; and exploring vessel formation induced by *HMGA2* overexpression both in vitro and in vivo.

Setting: University research laboratory.

Patients: None.

Interventions: None.

Main Outcome Measures: The main outcome measures include vessel density in leiomyomas with *HMGA2* or *MED12* alteration; angiogenic factor expression in primary leiomyoma and in and in vitro cell model; and vessel formation in leiomyoma cells with *HMGA2* overexpression in vitro and in vivo.

Results: Angiogenic factors and receptors were significantly upregulated at mRNA and protein levels in HMGA2-LM. Specifically, HMGA2-LM exhibited increased expression of *VEGFA, EGF, bFGF, TGFa, VEGFR1,* and *VEGFR2* compared to MED12-LM and myometrium. Overexpression of *HMGA2* in MM and LM cell lines resulted in increased secretion of angiogenesis-associated factors. Secreted factors promoted human umbilical vein endothelial cell (HUVEC) migration, tube formation, and wound healing. *HMGA2* overexpression upregulated IGF2BP2 and pAKT, and silencing the *IGF2BP2* gene reduced pAKT levels and reduced HUVEC migration. Myometrial cells with stable *HMGA2* overexpression exhibited increased colony formation and cell growth in vitro and formed xenografts with increased blood vessels.

Reprint requests: Jian-Jun Wei, M.D., Department of Pathology, Northwestern University, Feinberg School of Medicine, 251 East Huron Street, Feinberg 7-334, Chicago, IL 60611 (jianjunwei@northwestern.edu).

Y.L. has nothing to disclose. W.Q. has nothing to disclose. B.B.G. has nothing to disclose. T.G. has nothing to disclose. D.C. has nothing to disclose. S.B. has nothing to disclose. J.J.K. has nothing to disclose. J.-J.W. has nothing to disclose.

Conclusions: HMGA2-LM have a high vasculature density, which likely contributes to tumor growth and disease burden of this leiomyoma subtype. HMGA2 plays an important role in angiogenesis and the involvement of IGF2BP2-mediated pAKT activity in angiogenesis, which provides a potential novel target for therapy for this subtype of LM.

Keywords

Leiomyoma; HMGA2; AKT pathway; angiogenesis; xenograft

Uterine leiomyomas (LM) are the most common benign neoplasm in reproductive-aged women, and up to 70% of women develop LM (1). Current medical therapies show no significant long-term benefits, and hundreds of thousands of patients with LM end up undergoing myomectomy or hysterectomy (2). Several driver gene mutations/alterations (including *MED12* [mediator complex subunit 12], *HMGA2* [high mobility group AT-hook 2], *FH* [fumarate hydratase], and *COL5/6)* have been identified in LM, with about 10%–15% of LM being due to *HMGA2* overexpression (3, 4). LM with different driver gene mutations seem to target different molecular pathways that determine LM growth behavior (3) and deserve further investigation. Previous studies and clinical observation demonstrated that LM with *HMGA2* overexpression (HMGA2-LM) tend to be larger, with an increased growth rate compared to those without *HMGA2* overexpression (5–7). Although many oncogenic properties of *HMGA2* in malignant tumors have been characterized (8), little is known about *HMGA2* in LM development and growth.

HMGA2-LM may not easily to be recognized from other usual type LM by histology, but *HMGA2* overexpression is commonly seen in LM variants of intravascular leiomyomatosis (9), hydropic leiomyoma (5), and lipoleiomyoma (10). All of these leiomyoma variants tend to have high vessel density and increased vessel proliferation (5) in comparison to usual-type LM. Usual-type LM are vascular-poor and slow-growing tumors. This difference has raised the interesting question as to whether HMGA2 promoted LM growth through regulation of vessel formation. Currently, no published data clearly describe the association of driver gene mutations with specific histologic features of LM. Therefore, identification of HMGA2-LM remains a challenge. By reviewing histology from LM with known gene alterations of *MED12* or *HMGA2* overexpression (11), we observed that HMGA2-LM were usually cellular and hypervascular, with a wide range of growth patterns. Global gene expression analysis between leiomyomas harboring different driver gene alterations showed that insulin-like growth factor 2 mRNA-binding protein 2 *(IGF2BP2)* and insulin-like growth factor 2 *(IGF2)* were significantly upregulated in HMGA2-LM (3). Another study demonstrated that *IGF2BP2* is directly regulated by HMGA2 (12) through binding to the AT-rich regulatory region located in the first intron. The association of tumor angiogenesis with *HMGA2* overexpression remains largely unknown.

In this study, we demonstrate higher vessel density and increased expression of angiogenic genes in HMGA2-LM compared to MED12-LM (*MED12*-mutated LM). Both in vitro and in vivo studies have shown that overexpression of *HMGA2* promotes expression and secretion of angiogenesis factors in *HMGA2*-overexpressed myometrial and leiomyoma cells, stimulating human umbilical vein endothelial cell (HUVEC) cell motility, migration,

proliferation, and vessel network formation. Finally, the important role of *IGF2BP2* in the HMGA2-driven angiogenesis is demonstrated.

MATERIALS AND METHODS

Tumor Tissue Collection

Human myometrial and leiomyoma tissues were collected from premenopausal women undergoing hysterectomy or myomectomy at Northwestern Memorial Hospital, which was approved by the Northwestern University Institutional Review Board (IRB number STU00018080). Written informed consent was obtained from each patient. A total of 27 HMGA2-LM and 24 MED12-LM (mutation confirmed by Sanger sequencing) with matched myometria were used for this study. Many HMGA2-LM were from myomectomy specimens, and only nine matched myometria were available for study. Patients taking hormonal contraceptives or gonadotropin-releasing hormone agonists/antagonists within 3 months of tissue collection were excluded from the study following the Institutional Review Board–approved protocol.

Tissue Microarrays and Immunohistochemistry

Formalin-fixed paraffin-embedded (FFPE) tissues of HMGA2-LM (n = 24) and MED12-LM (n = 24) were selected for each case, and 2-mm tissue cores were taken to create tissue microarrays (TMAs). Briefly, a hollow needle from the Manual Tissue Arrayer MTA-1 (Beecher Instruments) was used to remove 2-mm-diameter tissue cores from regions of the FFPE tissues, and then the tissue cores were inserted into a recipient paraffin block in a precisely spaced, array pattern. After setting the block on an uncharged slide overnight at 37°C, a preheated (70°C) slide was used to flatten the TMA surfaces. Then, the TMAs were sectioned at 4 μm. The first and last slides of each TMA were stained with hematoxylin and eosin (H&E) for quality assurance. Immunohistochemical (IHC) staining was done for human HMGA2, CD34, and Ki-67 and for mouse CD31. IHC procedures were performed on a Ventana Nexus automated system as described previously (11). Antibody information is summarized in Supplemental Table 1. Immunostains were scored semiquantitatively by percentage and intensity by two pathologists. Intensity was scored as negative (0), weak (1+), moderate (2+), or strong (3+), and the percentage of positive tumor cells was scored from 0% to 100%. Selected IHC markers were scanned by virtual digital means (13).

Reverse Transcription – Polymerase Chain Reaction

Total RNA from cell lines was isolated with TRIZOL reagents (Invitrogen, Carlsbad, CA), and RNA from formalin-fixed paraffin-embedded tumors (27 HMGA2-LM, 14 MED12-LM and matched MM) were extracted by High Pure FFPET RNA Isolation Kit (Roche) according to the manufacturer's protocol. RNA concentration was measured with the NanoDrop (ND-1000, Saarbrücken, Germany), and cDNA was synthesized from 1 μg of total RNA by PrimeScript RT Reagent kit (TaKaRa). Quantitative reverse transcription–polymerase chain reaction (RT-PCR) was performed using a SYBR green PCR mix (Applied Biosystems) in an Applied Biosystems 7900HT Real-Time PCR System. mRNA expression from each sample was calculated by normalization using endogenous control *GAPDH.* The

experiments were repeated in triplicate. Primer information is listed in Supplemental Table 2.

HMGA2 Constructs and Stable Overgrowth

Stable *HMGA2* overexpression was established in immortalized myometrial and leiomyoma cell lines. The human myometrial cell line myo-hTERT and the leiomyoma cell line DD-HLM cells were kindly provided by C. Mendelson (UT Southwestern) and A. Al Hendy (UIC), respectively. Myo-hTERT cells were grown in DMEM/F12 medium with 10% fetal bovine serum (FBS). *HMGA2* overexpression plasmids were obtained from Origene (Origene). Lentivirus was produced in HEK293T cells. For stable infection, 1×10^5 cells were plated in six-well plates with 2 mL of medium without antibiotics. After overnight incubation, the medium was replaced by 1 mL of Opti-MEM Reduced-Serum Medium (Gibco) containing 50 μL of concentrated lentiviral particles and 8 mg/mL of polybrene per well. Fresh medium containing 2 mg/mL of puromycin (Invitrogen, USA) was added to each well 24 hours later and then selected for 2 weeks.

Transient Transfection for RNA Interference

IGF2BP2 siRNA and control siRNA were purchased from Santa Cruz and used for transfecting cells with Lipofectamine 3000 (Invitrogen) according to the manufacturer's protocol. Briefly, 5×10^4 cells/well were plated into a six-well plate for 24 hours to reach 70% confluency. After diluting 6 μL siRNA (150 pmol) and 7.5 μL Lipofectamine 3000 reagent by using 250 μL Opti-MEM medium (Gibco Laboratories) separately, they were mixed and incubated for 5 minutes at room temperature. Then the siRNA-lipid complex was added to the medium, and the cells were incubated for 2 days at 37°C. The efficiency of *IGF2BP2* inhibition was assessed by Western blot.

Sodium Dodecyl Sulfate – Polyacryamide Gel Electrophoresis and Western Blotting

Myometrial and leiomyoma cells were lysed using RIPA lysis and extraction buffer with protease and phosphatase inhibitors (Thermo Fisher Scientific). The protein concentration was determined by BCA Protein Assay kit (Thermo Fisher Scientific). Equal amounts of proteins were separated by sodium dodecyl sulfate – polyacryamide gel electrophoresis (SDS-PAGE) and subsequently transferred to polyvinylidene difluoride (PVDF) membranes. Blots were sequentially incubated with 5% milk and the following primary antibodies: HMGA2, β-actin, IGF2BP2, pAKT, and AKT. Antibody information is summarized in Supplemental Table 1. After overnight incubation, the membranes were blotted by specific horseradish peroxidase – conjugated goat anti-rabbit or goat anti-mouse secondary antibodies (Bio-Rad and detected by a Western blotting detection kit (Advansta). All the unedited scans of Western blot are shown in Supplemental Figure 3. The experiments were repeated in triplicate.

Growth Curve and Colony Formation

To measure cellular proliferation, the WST-1 assay (Roche) was performed. In brief, 100 μL of cells were seeded at 10^3 cells/well in 96-well plates with culture medium. At indicated time points, 10 μL of WST-1 reagent was added to each well and then incubated for 3 hours

at 37°C. Absorbance values at 490 nm were determined with a Micro-plate Reader (Bio-Rad, Hercules, CA). Data were presented as the percentage of cell viability relative to that of the first day. For the clonogenic assay, single-cell suspensions were seeded in six-well plates and cultured for 3 weeks. Next, the medium was carefully aspirated, and cell colonies were prepared by fixation with methanol. Colonies were then stained by Crystal Violet, photographed, and scored. Colonies of more than 50 cells were counted as the surviving fraction. The experiments were repeated in triplicate.

Preparation of Conditioned Media and HUVEC Culture

For conditioned media (CM), equal amounts of LM and MM cells with or without *HMGA2* overexpression were cultured with serum-free media for 48 hours, and then the CM were stored at −70°C until use. HUVEC (kindly provided by Dr. W. Muller, NU) were cultured in Human Endothelial Medium (Gibco) plus 10% FBS.

HUVEC Tube Formation

The ability of HUVEC to form network structures when cultured in different CM was tested on a matrix of Matrigel basement membrane (BD). First, 60 μL/well of Matrigel was plated onto 96-well plates and incubated for 30 minutes at 37°C. A total of 1.0×10^4 HUVEC were resuspended in 100 μL of the different CM containing 10% FBS. After 4–6 hours of incubation at 37 °C, cells were stained using Calcein AM (Invitrogen) and tube-like structures were photographed using a fluorescence microscope (Olympus). The experiments were repeated in triplicate.

Transwell and Wound-Healing Assay

The cell migration assay was performed using the Transwell system (Corning Costar). HUVEC were harvested and suspended in serum-free medium, then 200 μL of cell suspension (1.0×10^5 cells) was added into the upper chamber. CM were supplemented with 10% FBS, and then 700 μL of the mixture was added into the lower chamber. After treatment for 4–6 hours, the nonmigrated cells were removed from the top of the insert membrane using cotton swabs. The migrated cells attached to the bottom side surface of the membrane were fixed with methanol and stained with 0.2% Crystal Violet. The successfully migrated cells were photographed under an Olympus light microscope and counted on average of five random fields per chamber. For the wound-healing assay, HUVEC were cultured to confluence in six-well plates. The monolayer was scratched using a 10 -μL pipette tip and then cultured under normal conditions. Migration distance at 0 and 12 hours was measured to determine the rate of cell migration for each group. The experiments were repeated in triplicate.

Angiogenesis Protein Array

The expression profiles of angiogenesis-related proteins were analyzed using the Proteome Profiler Human Angiogenesis Antibody Array (R&D Systems, which could detect the relative levels of 55 angiogenesis-related proteins simultaneously. The experiments were performed according to the manufacturer’s instructions and as previously reported (14). The membranes used chemiluminescence for visualization after standard immunoblotting

procedures. Membranes were scanned and quantified with ImageJ software (https://imagej.nih.gov/lj). The average intensity of the signal of the duplicate spots for each protein was determined and followed by background subtraction of the negative control spots on the membrane.

Xenograft Tumor Model

All animal experiments were performed with the approval of Institutional Animal Care and Use Committee (IACUC) at Northwestern University. Female NOD scid gamma (NSG, catalog no. 005557) mice (aged 4–6 weeks) were purchased from Jackson Laboratory and housed in a strict barrier environment for immunodeficient mice. The NSG mice were injected subcutaneously in bilateral flanks with control or *HMGA2*-overexpressed myo-hTERT cell suspensions (5×10^6 cells in 100 μL of phosphate-buffered saline solution) mixed with matrigel. A total of 13 controls (vector) and 14 test *(HMGA2* overexpression) xenografts were prepared. Euthanasia of mice was performed after 15 weeks of implantation, and graft size was measured. Graft volume was calculated according to the following formula: TV (cm^3) = $a \times b^2 \times \pi/6$, where a is the longest diameter and b is the shortest diameter. Hematoxylin and eosin staining and immunostains were performed on sections from embedded tissue samples.

Statistical Analysis

GraphPad Prism software was used for statistical analysis. Immunostain score data are presented as median and ranges for the entire xenograft samples. Other data are presented as mean and standard deviation. Student's *t*-test was used to determine statistical significance. A P value < .05 was considered statistically significant.

RESULTS

HMGA2-LM and Vessel Density

HMGA2-LM contained fewer fibroblasts with increased extracellular matrix density than MED12-LM. Tumor cells tended to have relatively small round/oval nuclei similar to those typically present in hydropic leiomyoma (5). In contrast, MED12-LM showed classical storiform thick bundles, and tumor cells demonstrated elongated and "cigar"-shaped nuclei. We therefore reviewed and selected those LM with specific histologic and nuclear features for *HMGA2* expression analysis. Among the candidate cases, LM with strong and diffuse immunoreactivity for HMGA2 (Fig. 1B) were selected as HMGA2-LM and included in this study. A total of 27 cases of HMGA2-LM, 14 cases of MED12-LM (mutation confirmed by Sanger sequencing), and 23 matched myometrium tissues (nine HMGA2-MM and 14 MED12-MM) were examined by real-time RT-PCR. HMGA2-LM had at least a 20- to 80-fold increase in *HMGA2* expression in comparison to MED12-LM and MM (Fig. 1C). These findings are consistent with results detected by immunohistochemistry (Fig. 1B). As illustrated in Figure 1A, HMGA2-LM are usually large, with tan–white cut surfaces. Further histological evaluation revealed that the most striking feature of HMGA2-LM was its high vasculature density of thin- and thick-walled vessels supported by immunostain for CD34 (Fig. 1D). When comparing vessel density, HMGA2-LM (n = 27) had significantly higher

total and thick-walled vessel densities than MED12-LM (n = 14) ($P < .01$ and $P < .001$) (Fig. 1E and 1F).

Angiogenic Factors in HMGA2-LM and MED12-LM and Human Angiogenesis Array Analysis in *HMGA2* Overexpression

We then measured the expression of nine angiogenesis-associated genes by real-time RT-PCR (Fig. 2A, Supplemental Table 2). A significant upregulation of *IGF2, bFGF, TNFα, VEGFA, VEGFR1,* and *VEGFR2* was observed in HMGA2-LM compared to MED12-LM and matched MM (Fig. 2B), except that *VEGFA* was higher in both HMGA-LM and HMGA2-MM. All six upregulated genes showed moderate to strong correlation with *HMGA2* expression (Fig. 2C). These findings suggest that *HMGA2* overexpression is associated with the upregulation of angiogenesis factors.

To investigate the role of *HMGA2* in the regulation of angiogenesis, stable *HMGA2* overexpression was established by *lenti-hmga2* into myo-hTERT cells (MM^{hmga2}) and DD-HLM (LM^{hmga2}) (Fig. 2D). Quantitative RT-PCR analysis revealed that MM^{hmga2} had a 1.5- to 10-fold increase in *VEGFA, VEGFR1, VEGR2, TGFβ, bFGF,* and *EGF* expression in comparison to controls (MM^{vector}) (Fig. 2E). Using the Human Angiogenesis Array, many angiogenic proteins were up-regulated in CM from LM^{hmga2} compared to LM^{vector} (Supplemental Fig. 1A). Upregulated pro-angiogenic factors included HB-EGF, CXCL16, Prolactin, EGF, NGR1-β1, VEGF-C, MMP-8, PD-ECGF, FGF-acidic, Endoglin, IL-1β, FGF-4, FGF-basic, and VEGFA; downregulated anti-angiogenic factors included TIMP-1 and Serpin B5 (Fig. 2F). Quantitative expression analysis of all 55 angiogenic factors is summarized in Supplemental Figure 1B.

HMGA2 Enhances Angiogenesis in Vitro

The role of HMGA2 in vessel formation was investigated by several functional assays using CM from cell lines with or without *HMGA2* overexpression. First, when collected CM was used for the endothelial cell tube formation assay, the number of complete network structures formed by HUVEC was significantly higher in the CM from MM^{hmga2} and LM^{hmga2} compared to the corresponding controls (LM^{vector} and MM^{vector}) (Figure 3A and 3B). Next, HUVEC motility and cell migration were measured using a transwell assay and the scratch-healing assay. Both MM^{hmga2} and LM^{hmga2} showed increased migration of HUVEC through the transwells (Fig. 3C and Supplemental Figure 2A), as well as increased cell motility in the scratch-healing assay (Fig. 3D and Supplemental Figure 2B). Thus, *HMGA2* overexpression in LM and MM promoted the release of factors that increase HUVEC motility and migration.

Insulin-like growth factor 2 mRNA binding protein 2 (*IGF2BP2*) plays an important role in recruiting endothelia by modulating IGF-mediated activation of the IGF type-I receptor on endothelial cells (15). Also, *IGF2BP2* is significantly upregulated in HMGA2-LM (3, 16). *HMGA2* overexpression in MM^{hmga2} and LM^{hmga2} cell lines resulted in increased levels of IGF2BP2 and pAKT compared to LM^{vector} and MM^{vector} cells (Fig. 3E and Supplemental Figure 3C). Silencing *IGF2BP2* resulted in reduced pAKT levels, but did not affect HMGA2 levels (Fig. 3F and Supplemental Fig. 3D). Silencing *IGF2BP2* in both MM^{hmga2} and

LM^{hmga2} cell lines resulted in CM that attenuated migration of HUVEC through transwells compared to CM from control siRNA–transfected MM^{hmga2} and LM^{hmga2} cells (Fig. 3G and 3H). These data indicate that IGF2BP2 could mediate the HMGA2-driven angiogenesis in MM and LM cells.

HMGA2 Promotes Myometrial Cell Growth and Vessel Formation in Vivo

To demonstrate the role of HMGA2 on angiogenesis in vivo, we used our previously established xenograft model of human myometrial and leiomyoma in mice (17). *HMGA2* overexpressed in MM cells (myo-hTERT) were used in this study. We first evaluated MM cell growth ex vivo by colony formation assay, WST-1 assay (Fig. 4A), and three-dimensional (3D) spheroid culture (Fig. 4B) (16). MM^{hmga2} showed a significantly greater colony formation and higher viability than that of MM^{vector} (Fig. 4A). In spheroid cultures, MM^{hmga2} had strong and diffuse immunoreactivity for HMGA2, whereas MM^{vector} showed weak immunoreactivity for HMGA2 (Fig. 4B). MM^{hmga2} also had a significantly higher Ki-67 proliferation index than MM^{vector} control (Fig. 4B).

Cell pellets (5×10^6) of MM^{hmga2} and MM^{vector} were prepared with Matrigel (see Materials and Methods) and implanted into the back subcutaneous soft tissue of NSG mice. A total of 13 controls (MM^{vector}) and 14 test (MM^{hmga2}) xenografts were prepared. Implants were palpable at 10 weeks and reached 5 mm in diameter by 12 weeks. Mice were euthanized at 15 weeks and xenografts were collected (Fig. 4C). The volume of MM^{hmga2} grafts was larger than that of MM^{vector} xenografts (Fig. 4C). As observed with hematoxylin and eosin staining, control and test xenografts revealed spindle cell morphology. Immunohistochemistry demonstrated higher immunoreactivity for HMGA2 in MM^{hmga2} than in MM^{vector} (Fig. 4F), and MM^{hmga2} xenografts had a significantly higher Ki-67 proliferation index than MM^{vector} xenografts (Fig. 4D and 4F). To evaluate the vessel density inside xenograft nodules, immunostaining for mouse CD31 was performed on all xenografts. As illustrated in Figure 4E and 4F, MM^{hmga2} had significantly more vasculature within xenografts than MM^{vector}. Vessel density at × 20 magnification ranged from 20 to 55 vessels per field in MM^{hmga2} xenografts and from 3 to 33 vessels per field in MM^{vector} xenografts. These findings further demonstrated that *HMGA2* is one of the potent functional genes in regulating and promoting angiogenesis within uterine smooth muscle cells.

DISCUSSION

HMGA2 is a nonhistone chromatin protein that enhances DNA replication by maintaining DNA architecture and regulating transcription factors (18). Its primary functions involve cellular growth and differentiation. Expression of *HMGA2* is mainly restricted to the embryonic stage and is nearly undetectable in adult tissues (19). On the other hand, adult tissues with aberrant *HMGA2* expression are readily encountered in neoplastic processes, thereby highlighting *HMGA2's* property as a driving factor of oncogenesis. Upregulation of *HMGA2* has been identified in numerous tumors, both epithelial and mesenchymal (19). For example, about 10%–15% of leiomyomas harbor *HMGA2* overexpression, largely contributed by gene rearrangement (11). Mas et al. demonstrated that overexpression of *HMGA2* could transform myometrial cells toward leiomyoma cells that, in vivo, were able

to develop into leiomyomata (20); thus indicating *HMGA2's* role in leiomyoma tumorigenesis. Zaidi et al. provided additional in vivo evidence that *HMGA2* overexpression in differentiated mesenchyme has a causal role in producing mesenchymal tumors (21). Furthermore, *HMGA2* expression was shown to be positively associated with human mesenchymal stem cell self-renewal and even to promote disease progression (22, 23). Rommel et al. showed that CD34-positive hematopoietic stem cells from healthy individuals and leukemic cells from cancer patients expressed higher levels of HMGA2 (24). Although multiple studies have investigated *HMGA2*'s relation to stem cells and its driving role as an oncogene in mesenchymal neoplasms, little knowledge is understood about *HGMA2*'s influence on angiogenesis.

Our previous work showed that nearly 80% of hydropic LM had *HMGA2* overexpression and had significantly higher vessel density than conventional and other variants of LM, in line with prior observations by Clement et al. (5, 25). Tumor cells overexpressing *HMGA2* are observed predominantly in cords, in concentrated around vessels, and comprising the walls of thick vasculature (Fig. 1). In addition, a cellular rim/perivascular layer of CD34 IHC-positive pericytes is seen in hydropic LM overexpressing *HMGA2* that is not seen in conventional LM (5). We theorized that these tumor- and vessel-supporting pericytes, possibly stem cells, could play a role in tumorigenesis by maintaining vascularity or tumor progenitor cells. Our prior findings thus led us to evaluate HMGA2 ‘s role in angiogenesis. To the best of our knowledge, this is the first study to investigate the association of HMGA2 and angiogenesis in a mesenchymal neoplasm, specifically uterine leiomyoma.

Because of the increased vascularization in HGMA2-LM tumors, we set out to study the role of HMGA2 in angiogenesis. In this study, we demonstrated that HMGA2 enhances the secretion of angiogenic factors, promotes HUVEC tube formation and motility/migration, increases levels of IGF2BP2 and pAKT, increases proliferation in MM spheroids, and increases angiogenesis in MM xenografts. The increased angiogenesis due to HMGA2 has been shown to occur in other systems. Zhu et al. demonstrated that knockdown of *HMGA2* impaired the angiogenic functions of mouse endothelial progenitor cells, and, in turn, upregulation of *HMGA2* improved angiogenic activity (26). In another study, knockdown of *HMGA2* in let-7 transgenic mice gave rise to tortuous retinal vessels and defective pericyte coverage (27). HMGA2 was even found to promote angiogenesis in oral squamous cell carcinoma (28). These findings together indicate that *HMGA2* overexpression plays a significant and positive role in vasculogenesis. The upregulation of angiogenesis-associated factors by HGMA2 was observed in MM and LM cells, implicating its role in upregulating angiogenesis. Others have shown similar associations between HMGA2 and angiogenic function. For instance, Zha et al showed that in gastric carcinoma cells HMGA2-bound DNA fragments enriched by ChIP include those involved in VEGF signaling and TGF-β signaling pathways (29). In another study, HMGA2 transcriptionally regulated angiogenesis-related genes *VEGF-A*, *VEGF-C*, and *FGF-2* in oral squamous cell carcinoma cell lines (28). This understanding of *HMGA2* highlights its potency as an oncogene driving angiogenesis on a molecular level in neoplastic cells.

We also observed that overexpression of *HMGA2* upregulated insulin-like growth factor binding protein 2 (IGF2BP2), as well as pAKT levels. Silencing *IGF2BP2* expression by

siRNA (in HMGA2-stable cells) reduced pAKT levels and partially blocked *HMGA2*-promoting angiogenesis, indicating that *HMGA2* promotes pAKT signaling and angiogenesis through IGF2BP2. This is consistent with a study in which IGF2BP2 promoted cancer cell proliferation by activating the PI3K/AKT pathway in pancreatic tumors (30). Several studies in different cell types also noted that *HMGA2* was associated with AKT/mTOR activity (31, 32). The AKT/mTOR signaling pathway plays an important role in angiogenesis by regulating multiple critical steps, including endothelial cell survival, migration, and capillary-like structure formation (33, 34). One study demonstrated that *IGF2BP2* is directly regulated by HMGA2 (12), binding to the AT-rich regulatory region located in the first intron. Moreover, it has been shown that nuclear factor–κB (NF-κB) binds to a site immediately adjacent to the AT-rich regulatory region and regulates *IGF2BP2* gene, cooperating with HMGA2 protein. HMGA2-LM can ultimately enhance pAKT activity (16). The HMGA2/IGF2BP2/AKT–mTOR axis provides mechanistic understanding of the increased angiogenesis observed in HMGA2-LM.

The increased angiogenesis observed in MM^{hmga2} xenografts accompanied by a significantly higher proliferation index (Ki-67 percentage) than MM^{vector} indicates with confidence that HMGA2 significantly regulates angiogenesis in uterine smooth muscle cells. To our knowledge, this is the first report that demonstrates HMGA2 promoting angiogenesis using in vivo models. We also previously observed prominent CD34-positive pericytes in HMGA2-LM (5). It is well known that vessel walls are lined with endothelial cells, the neovascular functions of which are supported by adjacent pericytes. A recent study suggested that HMGA2 is an essential architectural transcription factor for mesenchymal and pericyte differentiation, as well as self-renewal and tumorigenic capabilities (35). The differential role of pericytes in HMGA2-LM warrants further investigation.

In summary, our data reveal that HMGA2-LM have a high density of both thin- and thick-walled vessels, which likely contributes to the tumor growth and disease burden of this leiomyoma subtype. We demonstrated a direct role of *HMGA2* on angiogenesis and the involvement of IGF2BP2-mediated pAKT activity in angiogenesis. Our data suggest that inhibiting angiogenesis or targeting vessel formation in HMGA2-LM could have beneficial therapeutic implications for patients. This understanding of *HMGA2s* oncogenic potential is clinically relevant when considering that HMGA2-LM grow to large sizes with increased morbidity compared to other LM subtypes (3, 4, 11).

Supplementary Material

Refer to Web version on PubMed Central for supplementary material.

Acknowledgments:

We thank Stacy Ann Kujawa and Bella Shmaltsuyeva for technical support; and Northwestern University's Pathology Core Facility for providing a place to perform our immunohistochemistry staining.

Supported by a National Institutes of Health grant (NIH P01HD57877).

REFERENCES

1. Baird DD, Dunson DB, Hill MC, Cousins D, Schectman JM. High cumulative incidence of uterine leiomyoma in black and white women: ultrasound evidence. Am J Obstet Gynecol 2003;188:100–7. [PubMed: 12548202]
2. Farquhar CM, Steiner CA. Hysterectomy rates in the United States 1990–1997. Obstet Gynecol 2002;99:229–34. [PubMed: 11814502]
3. Mehine M, Kaasinen E, Heinonen HR, Makinen N, Kampjarvi K, Sarvilinna N, et al. Integrated data analysis reveals uterine leiomyoma subtypes with distinct driver pathways and biomarkers. Proc Natl Acad Sci U S A 2016; 113:1315–20. [PubMed: 26787895]
4. Makinen N, Kampjarvi K, Frizzell N, Butzow R,Vahteristo P. Characterization of MED12, HMGA2, and FH alterations reveals molecular variability in uterine smooth muscle tumors. Mol Cancer 2017;16:101. [PubMed: 28592321]
5. Griffin BB, Ban Y, Lu X, Wei JJ. Hydropic leiomyoma: a distinct variant of leiomyoma closely related to HMGA2 overexpression. Hum Pathol 2019;84: 164–72. [PubMed: 30292626]
6. Tallini G, Vanni R, Manfioletti G, Kazmierczak B, Faa G, Pauwels P, et al. HMGI-C and HMGI(Y) immunoreactivity correlates with cytogenetic abnormalities in lipomas, pulmonary chondroid hamartomas, endometrial polyps, and uterine leiomyomas and is compatible with rearrangement of the HMGI-C and HMGI(Y) genes. Lab Invest 2000;80:359–69. [PubMed: 10744071]
7. Gross KL, Neskey DM, Manchanda N, Weremowicz S, Kleinman MS, Nowak RA, et al. HMGA2 expression in uterine leiomyomata and myometrium: quantitative analysis and tissue culture studies. Genes Chromosomes Cancer 2003;38:68–79. [PubMed: 12874787]
8. Wu J, Liu Z, Shao C, Gong Y, Hernando E, Lee P, et al. HMGA2 overexpression-induced ovarian surface epithelial transformation is mediated through regulation of EMT genes. Cancer Res 2011;71:349–59. [PubMed: 21224353]
9. Ordulu Z, Nucci MR, Dal Cin P, Hollowell ML, Otis CN, Hornick JL, et al. Intravenous leiomyomatosis: an unusual intermediate between benign and malignant uterine smooth muscle tumors. Mod Pathol 2016;29:500–10. [PubMed: 26892441]
10. Pedeutour F, Quade BJ, Sornberger K, Tallini G, Ligon AH, Weremowicz S, et al. Dysregulation of HMGIC in a uterine lipoleiomyoma with a complex rearrangement including chromosomes 7,12, and 14. Genes Chromosomes Cancer 2000;27:209–15. [PubMed: 10612811]
11. Bertsch E, Qiang W, Zhang Q, Espona-Fiedler M, Druschitz S, Liu Y, et al. MED12 and HMGA2 mutations: two independent genetic events in uterine leiomyoma and leiomyosarcoma. Mod Pathol 2014;27:1144–53. [PubMed: 24390224]
12. Cleynen I, Brants JR, Peeters K, Deckers R, Debiec-Rychter M, Sciot R, et al. HMGA2 regulates transcription of the Imp2 gene via an intronic regulatory element in cooperation with nuclear factor-kappaB. Mol Cancer Res 2007;5: 363–72. [PubMed: 17426251]
13. Varghese F, Bukhari AB, Malhotra R, De A. IHC Profiler: an open source plugin for the quantitative evaluation and automated scoring of immunohisto-chemistry images of human tissue samples. PLoS One 2014;9:e96801.
14. Hagman H, Bendahl PO, Lidfeldt J, Belting M, Johnsson A. Protein array profiling of circulating angiogenesis-related factors during bevacizumab containing treatment in metastatic colorectal cancer. PLoS One 2018;13: e0209838.
15. Png KJ, Halberg N, Yoshida M, Tavazoie SF. A microRNA regulon that mediates endothelial recruitment and metastasis by cancer cells. Nature 2011; 481:190–4. [PubMed: 22170610]
16. Xie J, Ubango J, Ban Y, Chakravarti D, Kim JJ, Wei JJ. Comparative analysis of AKT and the related biomarkers in uterine leiomyomas with MED12, HMGA2, and FH mutations. Genes Chromosomes Cancer2018;57:485–94.
17. Qiang W, Liu Z, Serna VA, Druschitz SA, Liu Y, Espona-Fiedler M, et al. Down-regulation of miR-29b is essential for pathogenesis of uterine leiomyoma. Endocrinology 2014;155:663–9. [PubMed: 24424054]
18. Fusco A, Fedele M. Roles of HMGA proteins in cancer. Nat RevCancer2007; 7:899–910.

19. Rogalla P, Drechsler K, Frey G, Hennig Y, Helmke B, Bonk U, et al. HMGI-C expression patterns in human tissues. Implications for the genesis of frequent mesenchymal tumors. Am J Pathol 1996;149:775–9. [PubMed: 8780382]
20. Mas A, Cervello I, Fernandez-Alvarez A, Faus A, Diaz A, Burgues O, et al. Overexpression of the truncated form of High Mobility Group A proteins (HMGA2) in human myometrial cells induces leiomyoma-like tissue formation. Mol Hum Reprod 2015;21:330–8. [PubMed: 25542836]
21. Zaidi MR, Okada Y, Chada KK. Misexpression of full-length HMGA2 induces benign mesenchymal tumors in mice. Cancer Res 2006;66:7453–9. [PubMed: 16885341]
22. Kalomoiris S, Cicchetto AC, Lakatos K, Nolta JA, Fierro FA. Fibroblast growth factor 2 regulates high mobility group a2 expression in human bone marrow-derived mesenchymal stem cells. J Cell Biochem 2016;117: 2128–37. [PubMed: 26888666]
23. Wei J, Li H, Wang S, Li T, Fan J, Liang X, et al. let-7 Enhances osteogenesis and bone formation while repressing adipogenesis of human stromal/ mesenchymal stem cells by regulating HMGA2. Stem Cells Dev 2014;23: 1452–63. [PubMed: 24617339]
24. Rommel B, Rogalla P, Jox A, Kalle CV, Kazmierczak B, Wolf J, et al. HMGI-C, a member of the high mobility group family of proteins, is expressed in hematopoietic stem cells and in leukemic cells. Leuk Lymphoma 1997;26: 603–7. [PubMed: 9389367]
25. Clement PB, Young RH, Scully RE. Diffuse, perinodular, and other patterns of hydropic degeneration within and adjacent to uterine leiomyomas. Problems in differential diagnosis. Am J Surg Pathol 1992;16:26–32. [PubMed: 1309411]
26. Zhu S, Deng S, Ma Q, Zhang T, Jia C, Zhuo D, et al. MicroRNA-10A* and MicroRNA-21 modulate endothelial progenitor cell senescence via suppressing high-mobility group A2. Circ Res 2013;112:152–64. [PubMed: 23072816]
27. Zhou Q, Frost RJA, Anderson C, Zhao F, Ma J, Yu B, et al. let-7 Contributes to diabetic retinopathy but represses pathological ocular angiogenesis. Mol Cell Biol 2017;37:e00001–17.
28. Sakata J, Hirosue A, Yoshida R, Kawahara K, Matsuoka Y, Yamamoto T, et al. HMGA2 contributes to distant metastasis and poor prognosis by promoting angiogenesis in oral squamous cell carcinoma. IntJ Mol Sci 2019;20:2473.
29. Zha L, Wang Z, Tang W, Zhang N, Liao G, Huang Z. Genome-wide analysis of HMGA2 transcription factor binding sites by ChIP on chip in gastric carcinoma cells. Mol Cell Biochem 2012;364:243–51. [PubMed: 22246783]
30. Zhu Y, Xu J, Liang W, Li J, Feng L, Zheng P, et al. miR-98–5p Alleviated epithelial-to-mesenchymal transition and renal fibrosis via targeting hmga2 in diabetic nephropathy. Int J Endocrinol 2019;2019:4946181.
31. Yu KR, Park SB, Jung JW, Seo MS, Hong IS, Kim HS, et al. HMGA2 regulates the in vitro aging and proliferation of human umbilical cord blood-derived stromal cells through the mTOR/p70S6K signaling pathway. Stem Cell Res 2013;10:156–65. [PubMed: 23276696]
32. Tan L, Wei X, Zheng L, Zeng J, Liu H, Yang S, et al. Amplified HMGA2 promotes cell growth by regulating Akt pathway in AML. J Cancer Res Clin Oncol 2016;142:389–99. [PubMed: 26319392]
33. Fujikane R, Komori K, Sekiguchi M, Hidaka M. Function of high-mobility group A proteins in the DNA damage signaling for the induction of apoptosis. Sci Rep 2016;6:31714. [PubMed: 27538817]
34. Wang H, Jiang Z, Chen H, Wu X, Xiang J, Peng J. MicroRNA-495 inhibits gastric cancer cell migration and invasion possibly via targeting High Mobility Group AT-Hook 2 (HMGA2). Med Sci Monit 2017;23: 640–8. [PubMed: 28159956]
35. Zhong X, Liu X, Li Y, Cheng M, Wang W, Tian K, et al. HMGA2 sustains self-renewal and invasiveness of glioma-initiating cells. Oncotarget 2016;7: 44365–80. [PubMed: 27259253]

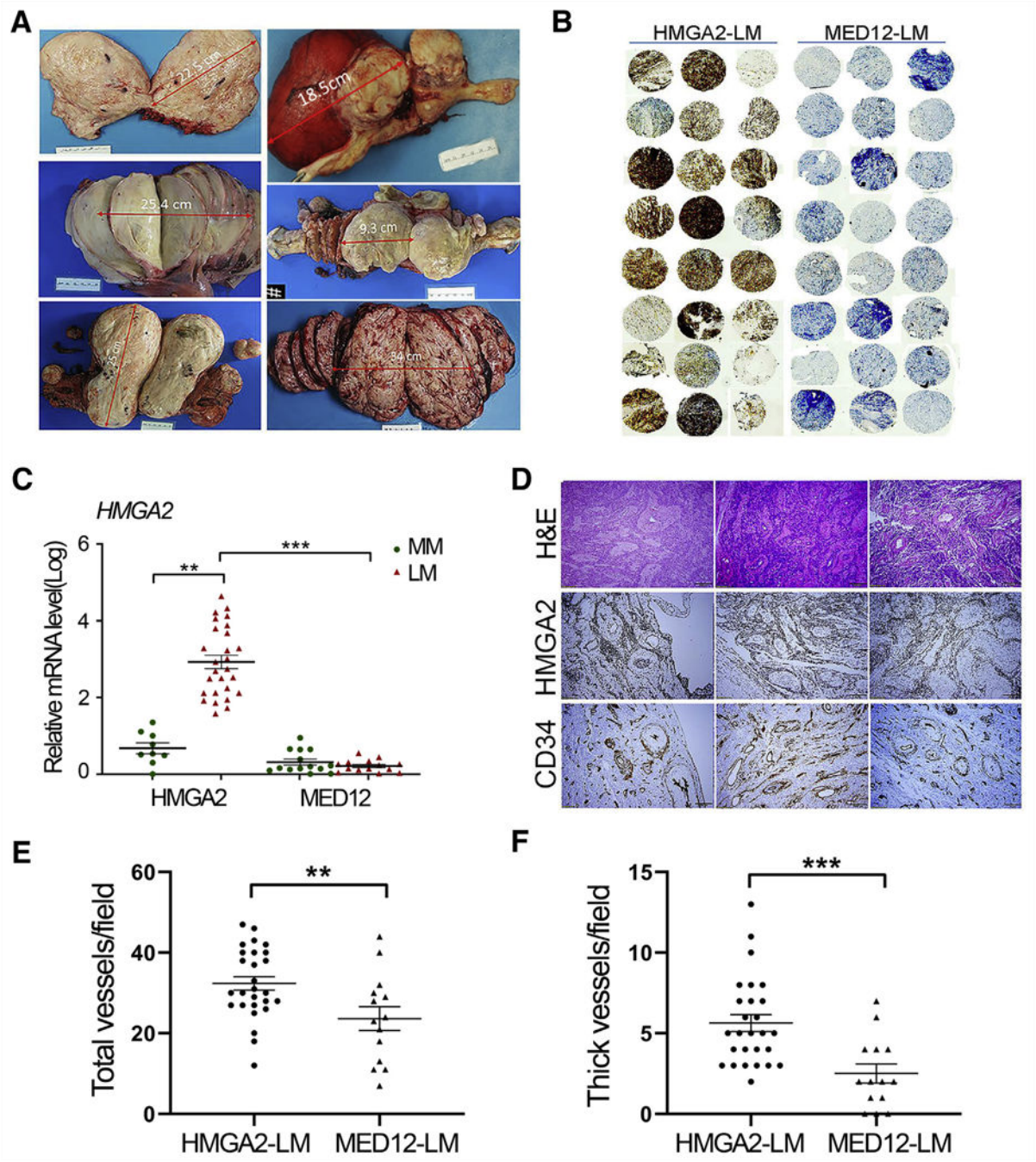

FIGURE 1.

HMGA2-LM and vessel density. (A) Examples of the gross appearance of HMGA2-LM. (B) Immunohistochemistry for HMGA2 in tissue microarray of HMGA2-LM (n = 24) and MED12-LM (n = 24). (C) Dot plot illustrating *HMGA2* expression in HMGA2-MM (n = 9), HMGA2-LM (n = 27), MED12-MM (n = 14), and MED12-LM (n = 14) detected by real-time reverse transcription–polymerase chain reaction (log ratio). (D) Examples of HMGA2-LM for histology by hematoxylin and eosin, HMGA2 overexpression (HMGA2 immunostain), and vessel distribution (CD34 immunostain). (E, F) Scatter plots illustrating

total vessel density (E) and specifically thick-walled vessel density (F) in HMGA2-LM (n = 27) versus MED12-LM (n = 14), counted under a microscope at ×10 magnification. *P<.05; **P<.01; ***P<.001.

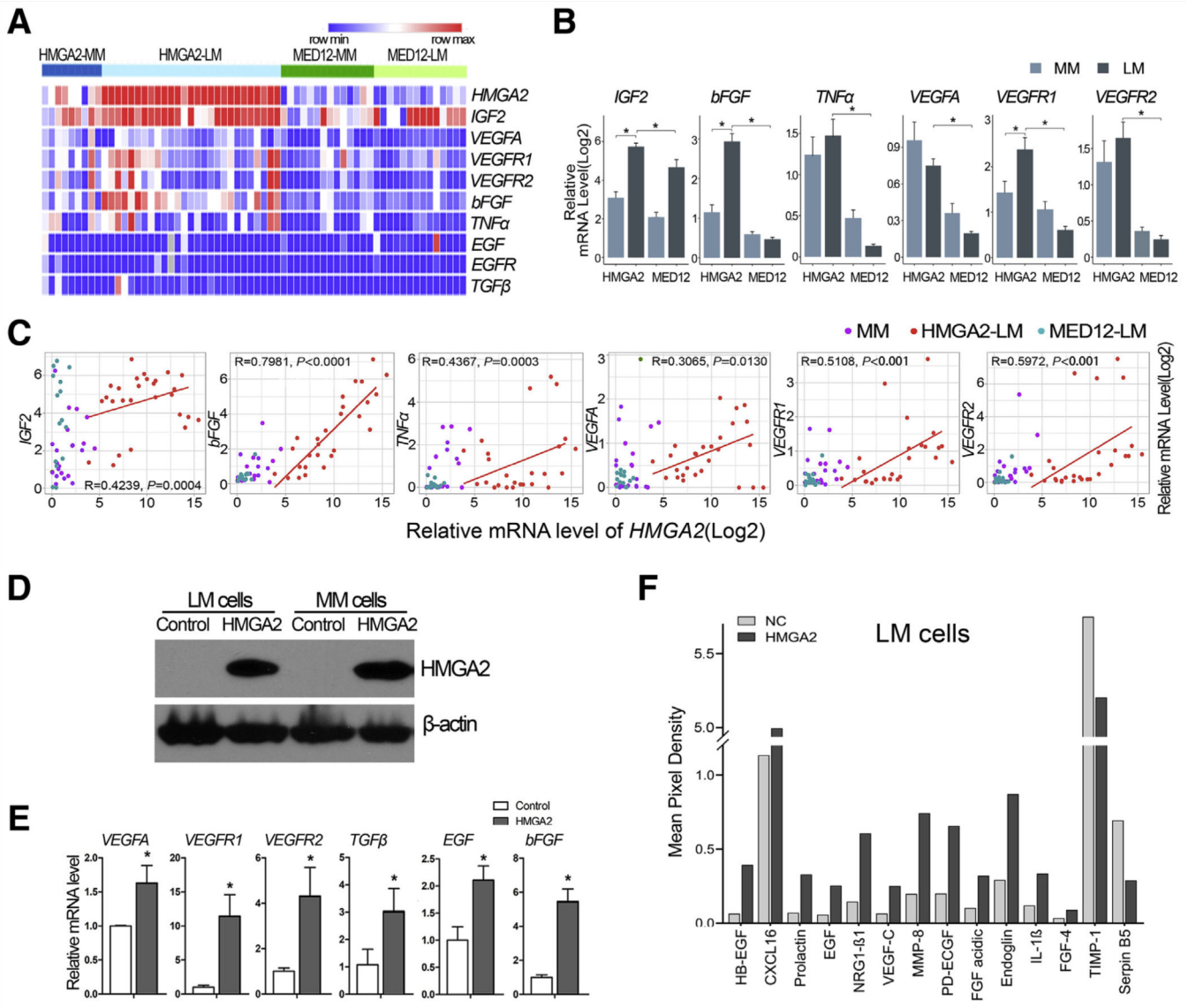

FIGURE 2.

Angiogenic factors in HMGA2-LM and MED12-LM and angiogenic factor array analysis in cell lines with stable *HMGA2* overexpression. (A, B) Heatmap and histograms showing relative expression of nine select angiogenic factors in HMGA2-MM (n = 9), HMGA2- LM (n = 27), MED12-MM (n = 14), and MED12- LM (n = 14). (C) Correlation analysis of *HMGA2* expression with six angiogenic factors. **P*<.05; ***P*<.01; ****P*<.001. (D) Western blot illustrating stable *HMGA2* overexpression. (E) Expression analysis of select angiogenic factor mRNA levels by reverse transcription–polymerase chain reaction in cell lines with stable *HMGA2* overexpression versus control cells. **P*<.05 (F) Histogram illustrating angiogenesis-related proteins production in LM cells with and without *HMGA2* overexpression.

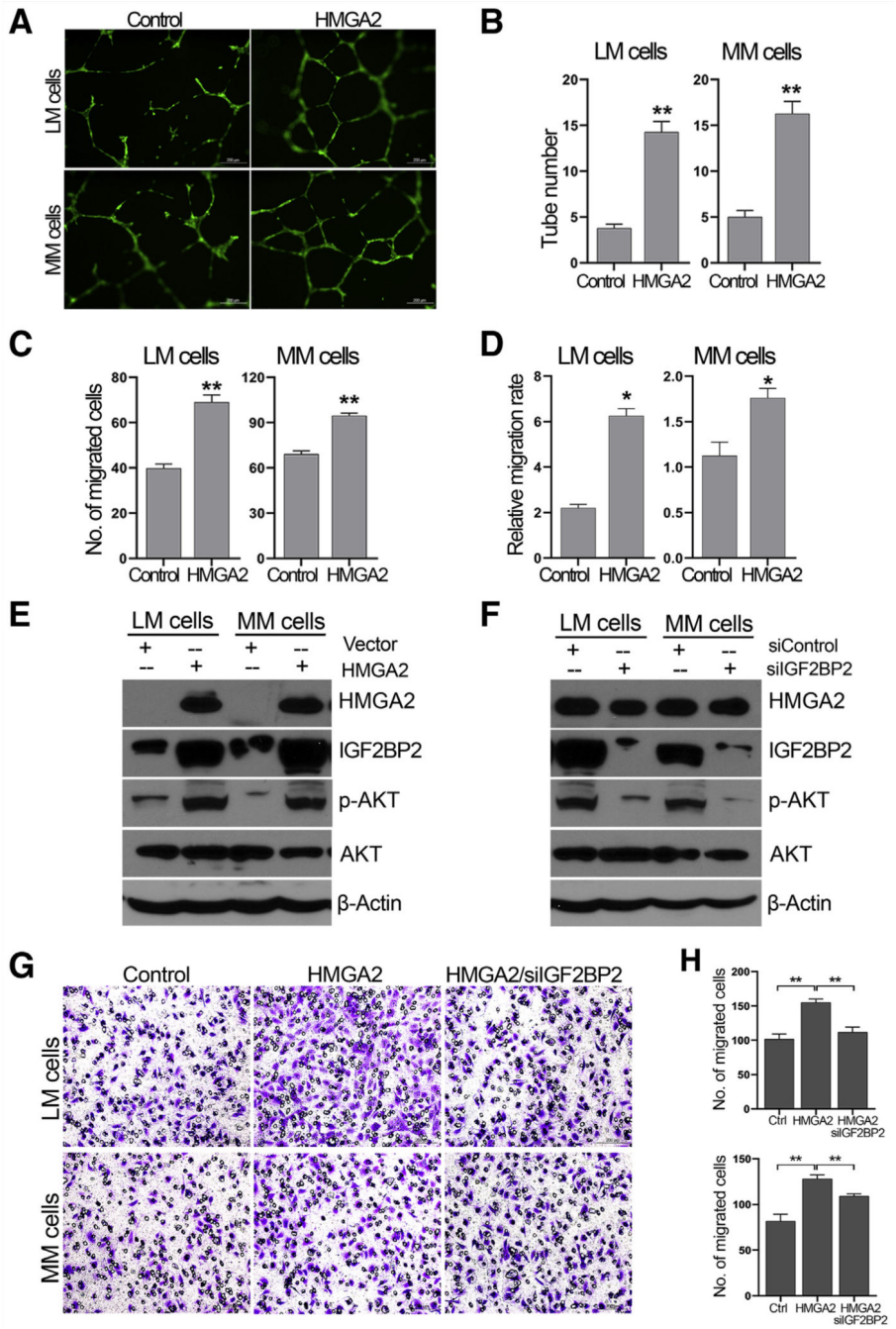

FIGURE 3.

HMGA2 promotes angiogenesis and mediates IGF2BP2/pAKT activity in human umbilical vein endothelial cell (HUVEC) migration. (A) Tube formation of HUVEC in the CM from LM and MM cells without (control) and with *HMGA2* overexpression. (B) Histogram demonstrating the number of complete tubes and significance analysis. (C) Histogram showing the number of migrated HUVEC (Transwell assay) in the CM from LM and MM cells without (control) and with *HMGA2* overexpression. (D) Histogram showing the relative migration rate of HUVEC after scratching in the CM from LM and MM cells

without (control) and with *HMGA2* overexpression. *P<.05; **P<.01. (E) Western blot analysis illustrating pAKT and IGF2BP2 expression in LM and MM cells with and without *HMGA2* overexpression. (F) Expression analysis of HMGA2 and pAKT in LM and MM cells after silencing *IGF2BP2* expression. (G, H) HUVEC migration analysis in the CM from LM and MM cells without (control) and with *HMGA2* overexpression, as well as silencing *IGF2BP2.*

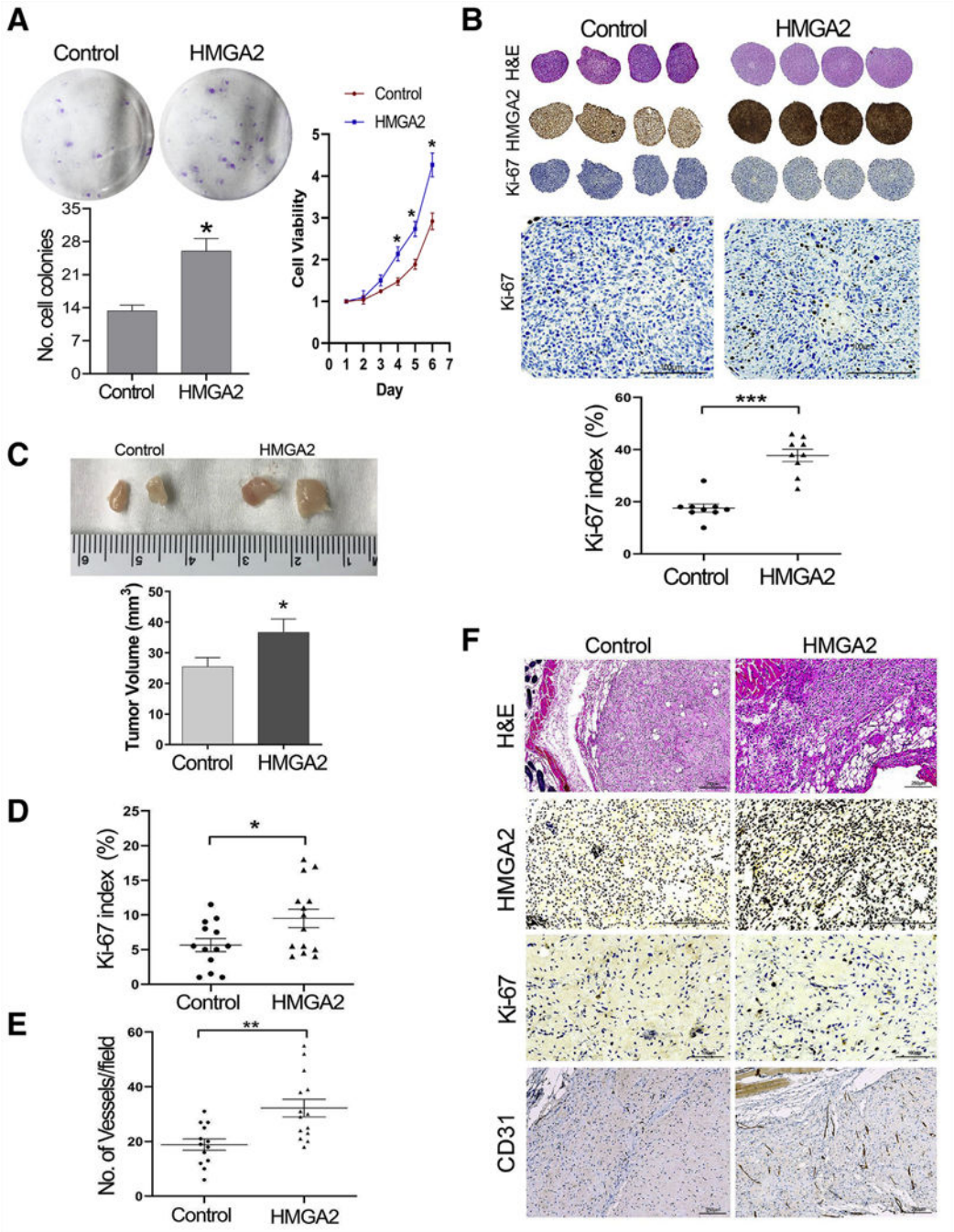

FIGURE 4.

Colony formation, WST-1 assay, spherical culture, and mouse xenografts of myometrial cells with *HMGA2* overexpression. (A) Colony formation (left) and WST-1 (right) in MM cell line with and without *HMGA2* overexpression. (B) Three-dimensional (3D) ex vivo spheroids (see Materials and Methods) were sectioned and examined in routine hematoxylin and eosin and immunostainsfor HMGA2 and Ki-67 (enlarged images to better view of Ki-67 positive cells). Dot plot showing the cell proliferation index (Ki-67 count) in nine spheroids of myometrial cell lines with and without *HMGA2* overexpression. **P*<.05; ****P*<.001. (C)

Examples of the dissected xenografts of myometrial cells with and without *HMGA2* overexpression from NOD scid gamma (NSG) mice and the volume of MM^{hmga2} (n = 14) and MM^{vector} (n = 13) xenografts at time of collection. (D, E) Ki-67 index and number of vessels detected by mouse CD31 in xenografts of MM^{hmga2} and MM^{vector}. $*P<.05$; $**P<.01$. (F) Examples of xenograft sections examined by hematoxylin eosin and immunostains for HMGA2 expression, Ki-67 (cell proliferation marker), CD31 (highlighted vessels) in MM^{hmga2}, and MM^{vector} are illustrated.